HHS Public Access

Author manuscript

Aquat Toxicol. Author manuscript; available in PMC 2016 April 01.

Published in final edited form as:

Aquat Toxicol. 2015 April ; 161: 221–230. doi:10.1016/j.aquatox.2015.02.009.

Triphenyl phosphate-induced developmental toxicity in zebrafish: Potential role of the retinoic acid receptor

Gregory M. Isales[a], **Rachel A. Hipszer**[a], **Tara D. Raftery**[a], **Albert Chen**[b], **Heather M. Stapleton**[b], and **David C. Volz**[a,*]

David C. Volz: volz@mailbox.sc.edu

[a]Department of Environmental Health Sciences, Arnold School of Public Health, University ofSouth Carolina, Columbia, SC USA

[b]Division of Environmental Sciences and Policy, Nicholas School of the Environment, DukeUniversity, Durham, NC USA

Abstract

Using zebrafish as a model, we previously reported that developmental exposure to triphenyl phosphate (TPP) – a high-production volume organophosphate-based flame retardant – results in dioxin-like cardiac looping impairments that are independent of the aryl hydrocarbon receptor. Using a pharmacologic approach, the objective of this study was to investigate the potential role of retinoic acid receptor (RAR) – a nuclear receptor that regulates vertebrate heart morphogenesis – in mediating TPP-induced developmental toxicity in zebrafish. We first revealed that static exposure of zebrafish from 5-72 hours post-fertilization (hpf) to TPP in the presence of non-toxic concentrations of an RAR antagonist (BMS493) significantly enhanced TPP-induced toxicity (relative to TPP alone), even though identical non-toxic BMS493 concentrations mitigated retinoic acid (RA)-induced toxicity. BMS493-mediated enhancement of TPP toxicity was not a result of differential TPP uptake or metabolism, as internal embryonic doses of TPP and diphenyl phosphate (DPP) – a primary TPP metabolite - were not different in the presence or absence of BMS493. Using real-time PCR, we then quantified the relative change in expression of cytochrome P450 26a1 *(cyp26a1)* – a major target gene for RA-induced RAR activation in zebrafish – and found that RA and TPP exposure resulted in a ∼5-fold increase and decrease in *cyp26a1* expression, respectively, relative to vehicle-exposed embryos. To address whether TPP may interact with human RARs, we then exposed Chinese hamster ovary cells stably transfected with chimeric human RARα-, RARβ-, or RARγ to TPP in the presence of RA, and found that TPP significantly inhibited RA-induced luciferase activity in a concentration-dependent manner. Overall, our findings suggest that zebrafish RARs may be involved in mediating TPP-induced developmental toxicity, a mechanism of action that may have relevance to humans.

*Corresponding author. Tel: +1 803 777 0218; fax: +1 803 777 3391.

The authors declare no conflicts of interest.

Keywords

retinoic acid receptor; flame retardant; triphenyl phosphate; zebrafish

1. Introduction

Triphenyl phosphate (TPP) is an unsubstituted aryl phosphate ester historically used as a high-production volume flame retardant within polyvinyl chloride, polymers, printed circuit boards, photographic films, and hydraulic fluids (Brooke et al., 2009). Based on estimates from 10-15 years ago, the combined production and use of TPP within Western Europe was 20,000-30,000 tons (or 44-66 million pounds) in 2000, while the combined production and use of TPP within the United States alone was 4,500-22,700 tons (or 10-50 million pounds) (van der Veen and de Boer, 2012). Since 2005, the use of TPP as a flame retardant within polyurethane foam likely increased within the United States following the phase-out of pentabrominated diphenyl ether and subsequent replacement with alternative TPP-containing flame retardant formulations (USEPA, 2005a). Similar to pentabrominated diphenyl ether, TPP is an additive flame retardant that can migrate from end-use products into indoor and outdoor environmental media (van der Veen and de Boer, 2012). As such, environmental exposure to TPP may pose a health risk to humans and ecological species, particularly during sensitive windows of development.

Using zebrafish embryos, we recently evaluated the potential developmental toxicity of brominated and aryl phosphate components (including TPP) present within Firemaster 550 (McGee et al., 2013), an increasingly used alternative formulation for polyurethane foam. Within this study, exposure to TPP and mono-isopropylated triaryl phosphate – but not the remaining brominated and aryl phosphate components of Firemaster 550 – blocked normal looping of the atrium and ventricle, resulting in a “tube heart” phenotype. In addition, heart malformations resulting from mono-isopropylated triaryl phosphate exposure – but not TPP exposure – were blocked in the presence of an aryl hydrocarbon receptor (AHR) antagonist (1-methyl-*N*-[2-methyl-4-[2-(2-methylphenyl)diazenyl]phenyl-1*H*-pyrazole-5-carboxamide, or CH223191). Therefore, since TPP-induced malformations appear to be AHR-independent, it is currently unclear how TPP induces developmental toxicity in zebrafish and whether this mechanism of action is conserved within other vertebrates.

Although TPP is known to activate human pregnane X receptor (Honkakoski et al., 2004; Kojima et al., 2013) and peroxisome proliferator-activated receptor γ (Belcher et al., 2014; Pillai et al., 2014), these two receptors are not known to play a major role in regulating cardiac development within vertebrates. However, retinoic acid receptor (RAR) is a ligand-activated nuclear receptor that (1) directly controls heart morphogenesis in zebrafish (Stainier and Fishman, 1992) and mice (Niederreither et al., 2001); (2) when over-activated by excess retinoic acid (RA), blocks normal cardiac looping within zebrafish (Chen et al., 2008); and (3) is activated by structurally diverse xenobiotics (Kamata et al., 2008). While mammals have three RAR orthologs (RARα-, RARβ-, and RARγ) (Bastien and Rochette-Egly, 2004), zebrafish lack RARβ and possess two different paralogs of RARα *(raraa* and *rarab)* and RARγ *(rarga* and *rargb)* (Waxman and Yelon, 2007). Despite these differences, cytochrome P450 26a1 *(cyp26a1)* is a major target gene for RA-induced RAR activation in

zebrafish (White et al., 1996), mice (Ray et al., 1997), and humans (White et al., 1997), representing a biomarker for assessing potential RAR activation *in vivo*.

Based on our previous findings relative to data available within the literature, the overall objective of this study was to begin investigating the potential role of RAR in mediating TPP-induced developmental toxicity in zebrafish. To accomplish this objective, we relied on a combination of high-content screening assays, real-time PCR, and human RAR reporter assays to test the hypothesis that TPP-mediated RAR activation results in developmental toxicity, a mechanism that, similar to our findings with mono-isopropylated triaryl phosphate (McGee et al., 2013), may have relevance to humans. We also quantified internal embryonic doses of TPP and diphenyl phosphate (DPP) – a primary TPP metabolite – to confirm uptake of TPP and determine whether TPP and DPP doses were affected by the presence of an RAR antagonist.

2. Materials and methods

2.1. Animals

For all assays described below, we relied on a robust line of transgenic zebrafish (*fli1:egfp*) that stably express enhanced green fluorescent protein within vascular endothelial cells (Lawson and Weinstein, 2002). Although we did not assess the potential impacts of chemical exposure on angiogenesis within this study, we relied on fluorescent *fli1:egfp* zebrafish to analyze heart rate and body length using previously optimized protocols (Yozzo et al., 2013). Adult *fli1:egfp* zebrafish were maintained on a 14-h:10-h light:dark cycle within a five-shelf stand-alone system (Aquatic Habitats, Inc., Apopka, FL, USA) containing photoperiod light-cycle enclosures and recirculating conditioned reverse osmosis water. Dissolved oxygen, pH, conductivity, salinity, alkalinity, and temperature within recirculating water were maintained at 4-6 mg/L, 6.5-7.5, 425-475 μS, <1 ppt, 50-100 mg/L, and 27-28°C, respectively; in addition, levels of ammonia, nitrite, and nitrate within recirculating water were consistently below 0.1 mg/L, 0.05 mg/L, and 2 mg/L, respectively. Adult females and males were bred directly on-system using in-tank breeding traps suspended within 3-L tanks, or bred off-system within a light- and temperature-controlled incubator using breeding traps suspended within 1-L tanks. For all experiments described below, newly fertilized eggs were staged according to previously described methods (Kimmel et al., 1995). All fish were handled and treated in accordance with approved Institutional Animal Care and Use Committee protocols at the University of South Carolina – Columbia.

2.2. Chemicals

TPP (99.5% purity) was purchased from ChemService, Inc. (West Chester, PA, USA), whereas all-*trans*-RA (99.7% purity) and 4-[(1*E*)-2-[5,6-dihydro-5,5-dimethyl-8-(2-phenylethynyl)-2-naphthalenyl]ethenyl]benzoic acid (BMS493, 98.2% purity) were purchased from R&D Systems (Minneapolis, MN, USA). Stock solutions of each chemical were prepared by dissolving chemicals in high performance liquid chromatography-grade dimethyl sulfoxide (DMSO) (50 mM), and then performing two-fold serial dilutions into DMSO to create stock solutions for each working solution. All stock solutions were stored at

room temperature within 2-mL amber glass vials containing polytetrafluoroethylene-lined caps. Working solutions of tricaine methanesulfonate (MS-222) (Western Chemical, Inc., Ferndale, WA, USA) were freshly prepared by dissolving MS-222 into embryo media (5 mM NaCl, 0.17 mM KCl, 0.33 mM $CaCl_2$, 0.33 mM $MgSO_4$), and working solutions of all treatments were freshly prepared by spiking stock solutions into embryo media, resulting in 0.1% DMSO within all vehicle control and treatment groups.

2.3. High-content screening assays with RA, TPP, and BMS493

2.3.1. Exposure setup—Black 384-well microplates containing 0.17-mm glass-bottom wells (Matrical Bioscience, Spokane, WA, USA) were used for all high-content screening assays. Immediately following spawning, newly fertilized eggs were collected and placed in groups of approximately 50 per plastic petri dish within a light- and temperature-controlled incubator until 5 hours post-fertilization (hpf). For each assay, 384 viable *fli1:egfp* embryos were arrayed at 5 hpf into a 384-well plate (one embryo per well; 32 embryos per treatment) containing 50 μL per well of vehicle (0.1% DMSO) or treatment solution (0.1-100 nM RA; 0.05-50 μM TPP; or 0.05-50 μM BMS493), and then incubated at 28°C under a 14-h:10-h light:dark cycle and static conditions until 72 hpf.

2.3.2. Image acquisition—At 72 hpf, the plate was removed from the incubator, and zebrafish embryos were anesthetized with 100 mg/L MS-222 by adding 25 μL of 300 mg/L MS-222 to 50 μL of vehicle or treatment solution. The plate was then centrifuged at 200 rpm for 2 min to help orient hatched embryos into right or left lateral recumbency. Using automated image acquisition protocols and parameters previously optimized (Yozzo et al., 2013) for our ImageXpress Micro Widefield High-Content Screening System (Molecular Devices, Sunnyvale, CA, USA), each embryo was imaged to analyze the following endpoints: heart rate, pericardial area, and body length. During the entire image acquisition period, internal temperature within the ImageXpress Micro system was maintained between 25-27°C by removing panels on both sides of the ImageXpress Micro system and blowing air from left to right through the ImageXpress Micro with a portable fan; internal temperature was monitored and recorded at initiation and termination of each imaging protocol using a digital thermometer. Following completion of image acquisition, 72-hpf embryos were then euthanized by placing the plate at 4°C for 30 minutes.

2.3.3. Data extraction—Within MetaXpress 4.0.0.24 software (Molecular Devices, Sunnyvale, CA, USA), custom journal scripts for extraction of heart rate, pericardial area, and body length data were used as previously described (Yozzo et al., 2013). Prior to data extraction, stream acquisitions within each well were inspected within MetaXpress to assess embryo orientation and survival. Coagulated embryos, unhatched embryos, grossly malformed embryos, or developed embryos lacking a heartbeat were not included in the analysis. Using these criteria, only hatched and live embryos positioned in right or left lateral recumbency were analyzed. Interactive semi-automated journal scripts were used to isolate regions of interest and quantify heart rate and pericardial area, whereas a fully automated journal script was used to quantify body length. Examples of raw and analyzed images for each endpoint as well as additional details of the data extraction and analysis process have been previously described (Yozzo et al., 2013).

2.4. BMS493 co-exposures

We used a pan-RAR antagonist (BMS493) to determine whether TPP-induced developmental toxicity was RAR-dependent. Based on exposures described in Section 2.3 and using pericardial area as an endpoint, non-toxic BMS493 concentrations selected for co-exposure experiments were 0.19 and 0.39 μM. Using identical exposure set-up and image acquisition protocols described in Section 2.3, we exposed embryos to RA (25, 50, or 100 nM) or TPP (3.125, 6.25, or 12.5 μM) in the presence or absence of 0.19 or 0.39 μM BMS493. For TPP-BMS493 co-exposures, we extracted and analyzed data for pericardial area, as this endpoint represented a readily measurable biomarker for cardiac looping defects. For RA-BMS493 co-exposures, we manually quantified the distance from the caudal fin to the anteroposterior axis within MetaXpress (Fig. S1) since RA disrupted normal caudal fin development in the absence of detectable effects on heart rate and pericardial area.

2.5. Quantification of internal embryonic doses of TPP and DPP

To quantify internal embryonic doses of TPP and DPP, 5-hpf *fli1:egfp* embryos (20 embryos per well; six wells per treatment) were arrayed into a clear 48-well Falcon tissue culture plate (Corning Life Sciences, Tewksbury, MA, USA) containing 1 mL per well of vehicle (0.1% DMSO) or 12.5 μM TPP in the presence or absence of 0.39 μM BMS493. Embryos were incubated at 28°C under a 14-h:10-h light:dark cycle and static conditions until 72 hpf, and then euthanized with an overdose of MS-222. For each replicate pool (three per treatment), 30 72-hpf embryos were combined from two replicate wells into a 2-mL cryovial, immediately snap-frozen in liquid nitrogen, and stored at -80°C until analysis.

Immediately prior to extraction, samples were spiked with deuterated TPP (d_{15}-TPP) and deuterated DPP (d_{10}-DPP). Analytes were extracted and quantified using previously published methods (Dishaw et al., 2014; McGee et al., 2012). Briefly, tissue homogenates were sonicated three times in 1 mL acetonitrile for 20 min. Combined acetonitrile extracts were concentrated to dryness under N_2 at 35°C and reconstituted in 1:1 methanol:water. Prior to analysis, particulates were removed using a 0.2-μM nylon membrane. Tissue extracts were analyzed using liquid chromatography-tandem mass spectrometry (LC/MS-MS) on an Agilent 1200 series LC connected to an Agilent 6410B triple quadrupole MS detector equipped with an electrospray ionization source. Analytes were separated chromatographically on a Kinetex XB-C18 column (100 mm × 2.1 mm, 2.6 μm; Phenomenex) using a methanol-water gradient. Analytes were detected using multiple reaction monitoring in positive (TPP and d_{15}-TPP) and negative (DPP and d_{10}-DPP) ionization modes. Method detection limits (MDLs) were defined as three times the standard deviation of lab blanks (if present) or three times the noise. MDLs for TPP and DPP were 1.7 and 0.15 ng, respectively.

2.6. Total RNA isolation and real-time PCR

To assess the potential effects of RA and TPP on *cyp26a1* expression, 5-hpf *fli1:egfp* embryos (20 embryos per well; 12 wells per treatment) were arrayed into a clear 48-well Falcon tissue culture plate (Corning Life Sciences, Tewksbury, MA, USA) containing 1 mL per well of vehicle (0.1% DMSO), 100 nM RA, or 12.5 μM TPP. Embryos were incubated

at 28°C under a 14-h:10-h light:dark cycle and static conditions until 72 hpf, and then euthanized with an overdose of MS-222, immediately snap-frozen in liquid nitrogen, and stored at -80°C until RNA extraction procedures.

After combining three replicate wells per pool, four replicate pools of 60 72-hpf embryos per pool were homogenized in 2-mL cryovials using a PowerGen Homogenizer (Thermo Fisher Scientific, Waltham, MA, USA). Following homogenization, a SV Total RNA Isolation System (Promega, Madison, WI, USA) was used to extract total RNA from each replicate sample per manufacturer's instructions. First-strand cDNAs were generated from total RNA using oligo$(dT)_{15}$ primers and AMV Reverse Transcriptase (Promega, Madison, WI, USA) and stored at -20°C until use. *cyp26a1* and *18s rRNA* cDNAs were amplified using the following primers: *cyp26a1*, forward primer 5′-GATGCTCTGGAGCACTACATTC-3′, reverse primer 5′-GTTCTTGCTCGTCCGTCTTTAT -3′; and *18s rRNA*, forward primer, 5′-TCGCTAGTTGGCATCGTTTATG-3′, reverse primer 5′-CGGAGGTTCGAAGACGATCA-3′. *18s rRNA* was selected as an internal control because it is stably expressed throughout zebrafish embryogenesis (McCurley and Callard, 2008). Per manufacturer's instructions, approximately 150 ng of *cyp26a1* and *18s rRNA* cDNA was PCR amplified in duplicate using GoTaq qPCR Master Mix (Promega, Madison, WI, USA) and an Applied Biosystems 7900HT Fast Real-Time PCR System (Life Technologies, Grand Island, NY, USA). Real-time PCR reaction conditions were 2 min at 95°C followed by 45 cycles of 95°C for 30 s, 51°C for 30 s, and 72°C for 30 s. Relative quantitation of gene expression within each treatment was calculated using the comparative cycle threshold method as previously described (Jayasinghe and Volz, 2012).

2.7. Human RAR reporter assays

A cell-based human RAR-driven luciferase reporter assay developed and conducted by the Services Group within INDIGO Biosciences (State College, PA) was used to determine whether TPP antagonized RA-induced activation of human RARα, RARβ-, or RARγ. 9-*cis* RA was used as an agonist for RARα, whereas *all-trans* RA was used as an agonist for RARβ and RARγ. 4-[[[5,6-Dihydro-5,5-dimethyl-8-(3-quinolinyl)-2-naphthalenyl]carbonyl]amino]benzoic acid (BMS195614) was used as a reference antagonist for RARα, and 4-[6-[(2-methoxyethoxy)methoxy]-7-tricyclo[3.3.1.13,7]dec-1 -yl-2-naphthalenyl)benzoic acid (CD2665) was used as a reference antagonist for RARβ and RARγ. Concentrated TPP stock was serially diluted in DMSO to yield 3.1, 6.3, 13, 25, 50, and 100 mM working stocks, and concentrated reference antagonist stocks were serially diluted in DMSO to yield 0.0006, 0.002, 0.01, 0.04, 0.16, 0.63, 2.5, and 10 mM working stocks. Treatment solutions were prepared by diluting working stocks in INDIGO's proprietary culture media, resulting in 0.1% DMSO within all wells. For positive control wells, 9-*cis* or *all-trans* RA was added at a final concentration that increased luminescence by ∼80% relative to negative control wells. Treatment wells contained identical 9-*cis* or *all-trans* RA concentrations as positive control wells, but also contained TPP (3.1, 6.3, 13, 25, 50, or 100 μM), BMS195614 (0.0006, 0.002, 0.01, 0.04, 0.16, 0.63, 2.5, or 10 μM), or CD2665 (0.0006, 0.002, 0.01, 0.04, 0.16, 0.63, 2.5, or 10 μM).

For each treatment group, spiked culture media (100 μL) was dispensed into triplicate assay wells (using a white 96-well microplate) containing Chinese hamster ovary cells stably transfected with (1) expression vector containing the N-terminal GAL4 DNA binding domain fused to the ligand binding domain of human RARα-, RARβ-, or RARγ and (2) reporter vector containing a firefly luciferase gene functionally linked to the GAL4-specific upstream activation sequence. Following a 24-h incubation at 37°C under 5% carbon dioxide (CO_2), treatment media was discarded and, following one rinse with INDIGO's proprietary live cell multiplex buffer, live cell multiplex substrate was added to each well of the assay plate to assess cell viability. Following incubation at 37°C for 30 min, fluorescence was quantified to determine the relative number of live cells per well, and then live cell multiplex substrate was discarded and 100 μL of ONE-Glo Luciferase Assay Reagent (Promega, Madison, WI, USA) was added to each well of the assay plate. After a 5-min incubation at room temperature, luminescence was quantified using a Glomax 96 microplate luminometer (Promega, Madison, WI, USA). Mean fluorescence and luminescence (± standard deviation) values were calculated for each treatment group based on triplicate wells per treatment. For cell viability data, mean fluorescence for each treatment group was normalized to mean fluorescence for RA-only wells to determine the percent change in cell viability relative to positive control wells.

2.8. Statistical analyses

All statistical procedures were performed using SPSS Statistics 21. A general linear model (GLM) analysis of variance (ANOVA) ($\alpha = 0.05$) was used for all data derived from high-content screening assays, real-time PCR, analytical chemistry, and human RAR reporter assays, as these data did not meet the equal variance assumption for non-GLM ANOVAs. Pair-wise Tukey-based multiple comparisons of least square means were performed to identify significant treatment-related effects relative to vehicle controls, as well as BMS493-related effects relative to corresponding treatments without BMS493.

3. Results

3.1. RA, TPP, and BMS493 are toxic to developing zebrafish embryos

RA resulted in 56-72% survival following exposure to 0.78-50 nM, whereas exposure at the highest concentration (100 nM) resulted in <50% survival (Fig. 1A). Body length (Fig. 1B) and pericardial area (Fig. 1D) were also significantly decreased and increased, respectively, at 100 nM. However, RA exposure resulted in no effect on heart rate at all concentrations tested (Fig. 1C), and no effect on body length and pericardial area at concentrations ≤50 nM. A representative image of a 72-hpf embryo treated with 50 nM RA is provided in Fig. S2.

TPP resulted in <50% survival at the highest concentration tested (50 μM) (Fig. 2A), while body length was significantly decreased at 25 and 50 μM (Fig. 2B). Pericardial area was significantly increased in a concentration-dependent manner at concentrations >3.125 μM (Fig. 2D). However, similar to RA, TPP exposure resulted in no significant effects on heart rate at all concentrations tested (Fig. 2C). A representative image of a 72-hpf embryo treated with 12.5 μM TPP is provided in Fig. S2.

BMS493 was significantly more toxic than TPP, resulting in a steep concentration-dependent effect on survival and 100% mortality following exposure to >1.56 μM (Fig. 3A). While body length was not affected following exposure to ≤1.56 μM (Fig. 3B), BMS493 exposure resulted in a significant increase in pericardial area at concentrations ≥0.78 μM (Fig. 3D). Moreover, while pericardial area was not affected at 0.39 μM and lower, BMS493 exposure significantly decreased heart rate by 25-50 beats per minute (bpm) relative to vehicle controls at all concentrations except 0.05 and 0.78 μM (Fig. 3C). A representative image of a 72-hpf embryo treated with 1.56 μM BMS493 is provided in Fig. S2.

3.2. BMS493 enhances TPP-induced toxicity in zebrafish embryos

While exposure to 50 and 100 nM RA alone resulted in a decrease in percent survival and increase in distance from the caudal fin to the anteroposterior axis (Fig. 4A and B), non-toxic concentrations of BMS493 (0.19 and 0.39 μM) mitigated RA-induced mortality (≥75% survival across all co-exposures) and caudal fin malformations in a concentration-dependent manner (Fig. 4B). However, unlike RA, co-exposure of embryos to 3.125-12.5 μM TPP and non-toxic concentrations of BMS493 resulted in a significant increase in pericardial area (Fig. 4C and D) – an effect that was further enhanced by increasing BMS493 concentrations. Representative images of 72-hpf embryos treated with 100 nM RA or 12.5 μM TPP in the presence or absence of 0.39 μM BMS493 are provided in Fig. S3.

3.3. Co-exposure with BMS493 does not affect internal embryonic doses of TPP or DPP

Mean internal embryonic doses of TPP following a static 5-72-hpf exposure to vehicle (0.1% DMSO), 12.5 μM TPP, 0.39 μM BMS493, or 12.5 μM TPP + 0.39 μM BMS493 were 1.46, 443.44, 2.41, and 453.83 ng/30 embryos, respectively (Fig. 5). Mean internal embryonic doses of DPP within these same treatments were <MDL, 1.75, <MDL, and 0.93, respectively (Fig. 5). Although TPP doses were significantly higher in both TPP treatments relative to vehicle controls, there were no significant differences in TPP and DPP doses within the TPP-BMS493 co-exposure compared to TPP alone (Fig. 5). Therefore, the presence of non-toxic BMS493 concentrations within the exposure media did not affect internal doses of TPP and DPP within 72-hpf embryos.

3.4. TPP exposure decreases cyp26a1 expression in zebrafish embryos

As described in Section 3.2, co-exposure to BMS493 did not mitigate - but rather enhanced - TPP-induced developmental toxicity in zebrafish. As a result, we quantified the potential effect of RA and TPP on *cyp26a1* expression in order to (1) confirm that RA exposure resulted in an increase in *cyp26a1* expression and (2) test the hypothesis that TPP exposure decreased *cyp26a1* expression. Indeed, while RA exposure resulted in a ∼5-fold increase in *cyp26a1* expression (Fig. 6), TPP exposure resulted in a ∼5-fold decrease in *cyp26a1* expression (Fig. 6).

3.5. TPP inhibits RA-induced activation of human RARα-, RARβ-, and RARγ

Using Chinese hamster ovary cells stably transfected with chimeric human RARα-, RARβ-, or RARγ, TPP significantly inhibited RA-induced luciferase activity at 50 and 100 μM for human RARα and RARβ and 100 μM for human RARγ (Fig. 7). Cell viability (percent live

cells) was ≥86% across all three assays for reference antagonist exposures and all TPP concentrations except for the highest concentration (100 μM); within this TPP concentration, cell viability was ≥74% across all three assays (Table S1).

4. Discussion

Within this study, we found that TPP exposure was toxic to developing zebrafish embryos, albeit at high nominal aqueous concentrations. Although the toxicity of TPP within adult animals (including zebrafish) has been extensively evaluated (Brooke et al., 2009; Liu et al., 2012; Liu et al., 2013; USEPA, 2005b), to our knowledge the potential toxicity of TPP during early vertebrate development has received little attention. To date, only one prenatal developmental toxicity study and one fish early life-stage study using rats and fathead minnows, respectively, have reported adverse findings (Brooke et al., 2009; USEPA, 2005b). Within Sprague-Dawley rats, daily exposure to 690 mg/kg/day TPP (the highest dose tested) decreased dam body weight in the absence of teratogenic effects, suggesting that maternal metabolism mitigated *in utero* exposure via transformation of TPP into non-toxic metabolites. Within fathead minnows, TPP significantly decreased post-hatch (fry) survival at 230 μg/L (the highest concentration tested) in the absence of effects on embryo hatchability, body length, and eye development, suggesting that the highest TPP concentration tested was unable to penetrate the embryonic chorion during development. While our findings demonstrate that TPP is toxic to developing zebrafish embryos at higher concentrations (e.g., 12.5 μM TPP = 4,078 μg/L TPP), the acute or chronic risk of TPP to fish embryos and larvae within aquatic environments is likely negligible since short- and long-term surface water TPP concentrations are expected to be <10 μg/L (Brooke et al., 2009; USEPA, 2005b).

While administration of exogenous RA was highly toxic at nominal concentrations >50 nM, BMS493 was significantly more potent than TPP and required an approximately 30-fold lower nominal concentration to induce a similar magnitude of toxicity. Broadly classified as an RAR antagonist, BMS493 is a pan-RAR inverse agonist that, upon interaction with the RAR ligand-binding domain, represses RAR function and decreases expression of RAR target genes relative to basal transcriptional levels (Germain et al., 2009; le Maire et al., 2010). While we did not assess the specificity of BMS493 to zebrafish RARs, previous studies published nearly 15 years ago confirmed that BMS493 is a potent inhibitor of RA signaling *in vivo* within mouse, chick, and zebrafish embryos (Dupe and Lumsden, 2001; Grandel et al., 2002; Stafford and Prince, 2002; Wendling et al., 2000; Wendling et al., 2001). Therefore, in our study, BMS493- induced toxicity at higher concentrations was likely due to abolishment of endogenous RA signaling required for normal embryonic development and survival.

Based on our previously published findings (McGee et al., 2013), we hypothesized that aberrant activation of RAR may mediate TPP-induced developmental toxicity. Contrary to our hypothesis, co-exposure of developing embryos to TPP and non-toxic BMS493 concentrations significantly enhanced toxicity relative to TPP alone, even though BMS493 mitigated RA-induced malformations. In addition, while RA exposure increased *cyp26a1* expression by ∼5-fold, TPP exposure decreased *cyp26a1* expression by ∼5-fold, suggesting

that TPP may have repressed RAR function – either directly or indirectly – relative to basal levels within vehicle-exposed embryos. Similar to the effect of TPP on *cyp26a1* expression, our previous findings showed that exposure of zebrafish embryos to 4 μM TPP within glass beakers decreased *cyp1a* (a major AHR target gene) expression by ∼7-fold (McGee et al., 2013), suggesting that TPP may affect crosstalk between the AHR and RAR during embryogenesis. Indeed, available data within the published literature supports this hypothesis, as endogenous RA and normal RAR function are required for expression of AHR mRNA and proper embryonic development in mice and fish (Hayashida et al., 2004; Jacobs et al., 2011).

Within hepatocytes, TPP undergoes rapid enzyme-mediated hydrolysis and hydroxylation to form DPP and hydroxyl TPP metabolites, respectively (Sasaki et al., 1984; Su et al., 2014; Van den Eede et al., 2013). Urinary TPP and DPP concentrations were recently measured within several adult human populations (Hoffman et al., 2014a; Hoffman et al., 2014b; Meeker et al., 2013), and results from these studies suggest that DPP may be a reliable indicator of human TPP exposure within indoor environments. Therefore, for this study, we relied on DPP as an indicator of potential TPP metabolism within developing zebrafish embryos. To determine whether BMS493 interfered with TPP uptake and/or metabolism, we quantified internal embryonic doses of TPP and DPP in 72-hpf embryos following a 5-72-hpf static exposure to vehicle or TPP in the presence or absence of BMS493. Interestingly, co-exposure with non-toxic concentrations of BMS493 did not affect internal doses of TPP or DPP, suggesting that (1) TPP is not metabolized to DPP during the first 72 h of zebrafish embryogenesis and (2) enhanced toxicity in the presence of BMS493 was not due to higher TPP doses relative to TPP-alone exposures. Rather, these data support the conclusion that TPP and BMS493 act synergistically within zebrafish embryos, possibly via direct or indirect interactions with RAR-relevant pathways.

Finally, based on our findings in zebrafish, we hypothesized that TPP may antagonize RA-induced activation of human RARα, RARβ-, or RARγ. Using Chinese hamster ovary cells stably transfected with chimeric human RAR and luciferase reporter vectors, TPP significantly inhibited RA-induced luciferase activity in a concentration-dependent manner. Therefore, our data suggest that TPP has the potential to interact – albeit very weakly – with the ligand-binding domain of human RARα, RARβ-, or RARγ. TPP is an agonist for human estrogen receptor α, estrogen receptor β, pregnane × receptor, and peroxisome proliferator-activated receptor γ (Belcher et al., 2014; Honkakoski et al., 2004; Kojima et al., 2013; Pillai et al., 2014) as well as an antagonist for human androgen receptor and glucocorticoid receptor (Kojima et al., 2013). To our knowledge, this is the first study to identify TPP as a potential human RAR antagonist, supporting the emerging hypothesis that TPP – san industrial chemical that, unlike drugs and pesticides, was not designed to exhibit specificity and target a single class of receptors – may interact with multiple nuclear receptors localized within a diverse set of target tissues and organs.

In summary, our data collectively suggest that zebrafish RARs may be involved in mediating TPP-induced developmental toxicity, a mechanism of action that may have relevance to humans. However, we recognize that additional research is needed to (1) confirm that TPP-induced toxicity in zebrafish embryos is RAR-dependent; (2) identify

whether TPP-induced effects on *cyp26a1* expression are localized to target organs such as the developing heart; and (3) identify RAR-dependent and RAR-independent pathways that may be affected by TPP during embryogenesis. Therefore, future studies should rely on RAR-specific morpholino oligos, *cyp26a1*-specific whole-mount *in situ* hybridizations, and whole genome expression profiling to better clarify the role of RAR-relevant pathways in mediating developmental toxicity. Nevertheless, our current findings continue to highlight the complexity of deciphering mechanisms of developmental toxicity for organophosphate-based flame retardants such as TPP in zebrafish and other vertebrates.

Supplementary Material

Refer to Web version on PubMed Central for supplementary material.

Acknowledgments

Funding was provided in part by a South Carolina Honors College Science Undergraduate Research Fellowship to G.M.I., and a National Institutes of Health award (1R21ES022797-01A1), U.S. EPA Science to Achieve Results grant (R835169), and University of South Carolina Magellan Scholar grant to D.C.V. The contents of this manuscript are solely the responsibility of D.C.V. and do not necessarily represent the official views of the U.S. EPA. Further, the U.S. EPA does not endorse the purchase of any commercial products or services mentioned in the publication. We gratefully thank Dr. Robert Tanguay (Oregon State University) for providing founder fish to establish our *fli1:egfp* zebrafish colony; Dr. R. Sean Norman (University of South Carolina) for use of the Applied Biosystems 7900HT Fast Real-Time PCR System; and Drs. Prajakta Albrecht and Koji Toyokawa (INDIGO Biosciences) for providing human RAR reporter assay services.

References

Bastien J, Rochette-Egly C. Nuclear retinoid receptors and the transcription of retinoid-target genes. Gene. 2004; 328:1–16. [PubMed: 15019979]

Belcher SM, Cookman CJ, Patisaul HB, Stapleton HM. In vitro assessment of human nuclear hormone receptor activity and cytotoxicity of the flame retardant mixture FM 550 and its triarylphosphate and brominated components. Toxicol Lett. 2014; 228:93–102. [PubMed: 24786373]

Brooke, D.; Crookes, M.; Quarterman, P.; Burns, J. Environmental risk evaluation report: triphenyl phosphate (CAS no 115-86-6). Environment Agency; Bristol, UK: 2009. p. 140

Chen J, Carney SA, Peterson RE, Heideman W. Comparative genomics identifies genes mediating cardiotoxicity in the embryonic zebrafish heart. Physiol Genomics. 2008; 33:148–158. [PubMed: 18230668]

Dishaw LV, Hunter DL, Padnos B, Padilla S, Stapleton HM. Developmental exposure to organophosphate flame retardants elicits overt toxicity and alters behavior in early life stage zebrafish (Danio rerio). Toxicol Sci. 2014; 142:445–454. [PubMed: 25239634]

Dupe V, Lumsden A. Hindbrain patterning involves graded responses to retinoic acid signalling. Development. 2001; 128:2199–2208. [PubMed: 11493540]

Germain P, Gaudon C, Pogenberg V, Sanglier S, Van Dorsselaer A, Royer CA, Lazar MA, Bourguet W, Gronemeyer H. Differential action on coregulator interaction defines inverse retinoid agonists and neutral antagonists. Chem Biol. 2009; 16:479–489. [PubMed: 19477412]

Grandel H, Lun K, Rauch GJ, Rhinn M, Piotrowski T, Houart C, Sordino P, Kuchler AM, Schulte-Merker S, Geisler R, Holder N, Wilson SW, Brand M. Retinoic acid signalling in the zebrafish embryo is necessary during pre-segmentation stages to pattern the anterior-posterior axis of the CNS and to induce a pectoral fin bud. Development. 2002; 129:2851–2865. [PubMed: 12050134]

Hayashida Y, Kawamura T, Hori-e R, Yamashita I. Retionic acid and its receptors are required for expression of aryl hydrocarbon receptor mRNA and embryonic development of blood vessel and bone in the medaka fish, Oryzias latipes. Zoolog Sci. 2004; 21:541–551. [PubMed: 15170058]

Hoffman K, Daniels JL, Stapleton HM. Urinary metabolites of organophosphate flame retardants and their variability in pregnant women. Environ Int. 2014a; 63:169–172. [PubMed: 24316320]

Hoffman, K.; Garantziotis, S.; Birnbaum, LS.; Stapleton, HM. Environ Health Perspect. 2014b. Monitoring Indoor Exposure to Organophosphate Flame Retardants: Hand Wipes and House Dust.

Honkakoski P, Palvimo JJ, Penttila L, Vepsalainen J, Auriola S. Effects of triaryl phosphates on mouse and human nuclear receptors. Biochem Pharmacol. 2004; 67:97–106. [PubMed: 14667932]

Jacobs H, Dennefeld C, Feret B, Viluksela M, Hakansson H, Mark M, Ghyselinck NB. Retinoic acid drives aryl hydrocarbon receptor expression and is instrumental to dioxin-induced toxicity during palate development. Environ Health Perspect. 2011; 119:1590–1595. [PubMed: 21807577]

Jayasinghe BS, Volz DC. Aberrant ligand-induced activation of G protein-coupled estrogen receptor 1 (GPER) results in developmental malformations during vertebrate embryogenesis. Toxicol Sci. 2012; 125:262–273. [PubMed: 21984484]

Kamata R, Shiraishi F, Nishikawa J, Yonemoto J, Shiraishi H. Screening and detection of the in vitro agonistic activity of xenobiotics on the retinoic acid receptor. Toxicol In Vitro. 2008; 22:1050–1061. [PubMed: 18289828]

Kimmel CB, Ballard WW, Kimmel SR, Ullmann B, Schilling TF. Stages of embryonic development of the zebrafish. Dev Dyn. 1995; 203:253–310. [PubMed: 8589427]

Kojima H, Takeuchi S, Itoh T, Iida M, Kobayashi S, Yoshida T. In vitro endocrine disruption potential of organophosphate flame retardants via human nuclear receptors. Toxicology. 2013; 314:76–83. [PubMed: 24051214]

Lawson ND, Weinstein BM. In vivo imaging of embryonic vascular development using transgenic zebrafish. Dev Biol. 2002; 248:307–318. [PubMed: 12167406]

le Maire A, Teyssier C, Erb C, Grimaldi M, Alvarez S, de Lera AR, Balaguer P, Gronemeyer H, Royer CA, Germain P, Bourguet W. A unique secondary-structure switch controls constitutive gene repression by retinoic acid receptor. Nat Struct Mol Biol. 2010; 17:801–807. [PubMed: 20543827]

Liu X, Ji K, Choi K. Endocrine disruption potentials of organophosphate flame retardants and related mechanisms in H295R and MVLN cell lines and in zebrafish. Aquat Toxicol. 2012; 114-115:173–181. [PubMed: 22446829]

Liu X, Ji K, Jo A, Moon HB, Choi K. Effects of TDCPP or TPP on gene transcriptions and hormones of HPG axis, and their consequences on reproduction in adult zebrafish (Danio rerio). Aquat Toxicol. 2013; 134-135:104–111. [PubMed: 23603146]

McCurley AT, Callard GV. Characterization of housekeeping genes in zebrafish: male-female differences and effects of tissue type, developmental stage and chemical treatment. BMC Mol Biol. 2008; 9:102. [PubMed: 19014500]

McGee SP, Cooper EM, Stapleton HM, Volz DC. Early zebrafish embryogenesis is susceptible to developmental TDCPP exposure. Environ Health Perspect. 2012; 120:1585–1591. [PubMed: 23017583]

McGee SP, Konstantinov A, Stapleton HM, Volz DC. Aryl phosphate esters within a major PentaBDE replacement product induce cardiotoxicity in developing zebrafish embryos: potential role of the aryl hydrocarbon receptor. Toxicol Sci. 2013; 133:144–156. [PubMed: 23377616]

Meeker JD, Cooper EM, Stapleton HM, Hauser R. Urinary metabolites of organophosphate flame retardants: temporal variability and correlations with house dust concentrations. Environ Health Perspect. 2013; 121:580–585. [PubMed: 23461877]

Niederreither K, Vermot J, Messaddeq N, Schuhbaur B, Chambon P, Dolle P. Embryonic retinoic acid synthesis is essential for heart morphogenesis in the mouse. Development. 2001; 128:1019–1031. [PubMed: 11245568]

Pillai, HK.; Fang, M.; Beglov, D.; Kozakov, D.; Vajda, S.; Stapleton, HM.; Webster, TF.; Schlezinger, JJ. Environ Health Perspect. 2014. Ligand Binding and Activation of PPARgamma by Firemaster(R) 550: Effects on Adipogenesis and Osteogenesis.

Ray WJ, Bain G, Yao M, Gottlieb DI. CYP26, a novel mammalian cytochrome P450, is induced by retinoic acid and defines a new family. J Biol Chem. 1997; 272:18702–18708. [PubMed: 9228041]

Sasaki K, Suzuki T, Takeda M, Uchiyama M. Metabolism of phosphoric acid triesters by rat liver homogenate. Bull Environ Contam Toxicol. 1984; 33:281–288. [PubMed: 6478075]

Stafford D, Prince VE. Retinoic acid signaling is required for a critical early step in zebrafish pancreatic development. Curr Biol. 2002; 12:1215–1220. [PubMed: 12176331]

Stainier DY, Fishman MC. Patterning the zebrafish heart tube: acquisition of anteroposterior polarity. Dev Biol. 1992; 153:91–101. [PubMed: 1516755]

Su G, Crump D, Letcher RJ, Kennedy SW. Rapid in vitro metabolism of the flame retardant triphenyl phosphate and effects on cytotoxicity and mRNA expression in chicken embryonic hepatocytes. Environ Sci Technol. 2014; 48:13511–13519. [PubMed: 25350880]

USEPA. Design for the Environment. Washington, DC: 2005a. Furniture flame retardancy partnership: environmetnal profiles of chemical flame-retardant alternatives for low-density polyurethane foam.

USEPA. Design for the Environment. Washington, DC; 2005b. Furniture Flame Retardancy Partnership: Environmental Profiles of Chemical Flame-Retardant Alternatives for Low-Density Polyurethane Foam.

Van den Eede N, Maho W, Erratico C, Neels H, Covaci A. First insights in the metabolism of phosphate flame retardants and plasticizers using human liver fractions. Toxicol Lett. 2013; 223:9–15. [PubMed: 23994729]

van der Veen I, de Boer J. Phosphorus flame retardants: properties, production, environmental occurrence, toxicity and analysis. Chemosphere. 2012; 88:1119–1153. [PubMed: 22537891]

Waxman JS, Yelon D. Comparison of the expression patterns of newly identified zebrafish retinoic acid and retinoid X receptors. Dev Dyn. 2007; 236:587–595. [PubMed: 17195188]

Wendling O, Dennefeld C, Chambon P, Mark M. Retinoid signaling is essential for patterning the endoderm of the third and fourth pharyngeal arches. Development. 2000; 127:1553–1562. [PubMed: 10725232]

Wendling O, Ghyselinck NB, Chambon P, Mark M. Roles of retinoic acid receptors in early embryonic morphogenesis and hindbrain patterning. Development. 2001; 128:2031–2038. [PubMed: 11493525]

White JA, Beckett-Jones B, Guo YD, Dilworth FJ, Bonasoro J, Jones G, Petkovich M. cDNA cloning of human retinoic acid-metabolizing enzyme (hP450RAI) identifies a novel family of cytochromes P450. J Biol Chem. 1997; 272:18538–18541. [PubMed: 9228017]

White JA, Guo YD, Baetz K, Beckett-Jones B, Bonasoro J, Hsu KE, Dilworth FJ, Jones G, Petkovich M. Identification of the retinoic acid-inducible all-trans-retinoic acid 4-hydroxylase. J Biol Chem. 1996; 271:29922–29927. [PubMed: 8939936]

Yozzo KL, Isales GM, Raftery TD, Volz DC. High-content screening assay for identification of chemicals impacting cardiovascular function in zebrafish embryos. Environ Sci Technol. 2013; 47:11302–11310. [PubMed: 24015875]

Abbreviations

AHR	aryl hydrocarbon receptor
BMS493	4-[(1*E*)-2-[5,6-dihydro-5,5-dimethyl-8-(2-phenylethynyl)-2-naphthalenyl]ethenyl]benzoic acid
cyp26a1	cytochrome P450 26a1
DMSO	dimethyl sulfoxide
DPP	diphenyl phosphate
hpf	hours post-fertilization
MS-222	tricaine methanesulfonate
RA	retinoic acid

RAR	retinoic acid receptor
TPP	triphenyl phosphate

Highlights

- Triphenyl phosphate-induced toxicity in zebrafish embryos is enhanced in the presence of a retinoic acid receptor antagonist.
- Triphenyl phosphate uptake or metabolism within zebrafish embryos is not altered in the presence of a retinoic acid receptor antagonist.
- Triphenyl phosphate decreases expression of cytochrome P450 26a1 in zebrafish embryos.
- Triphenyl phosphate inhibits retinoic acid-induced activation of human retinoic acid receptors.

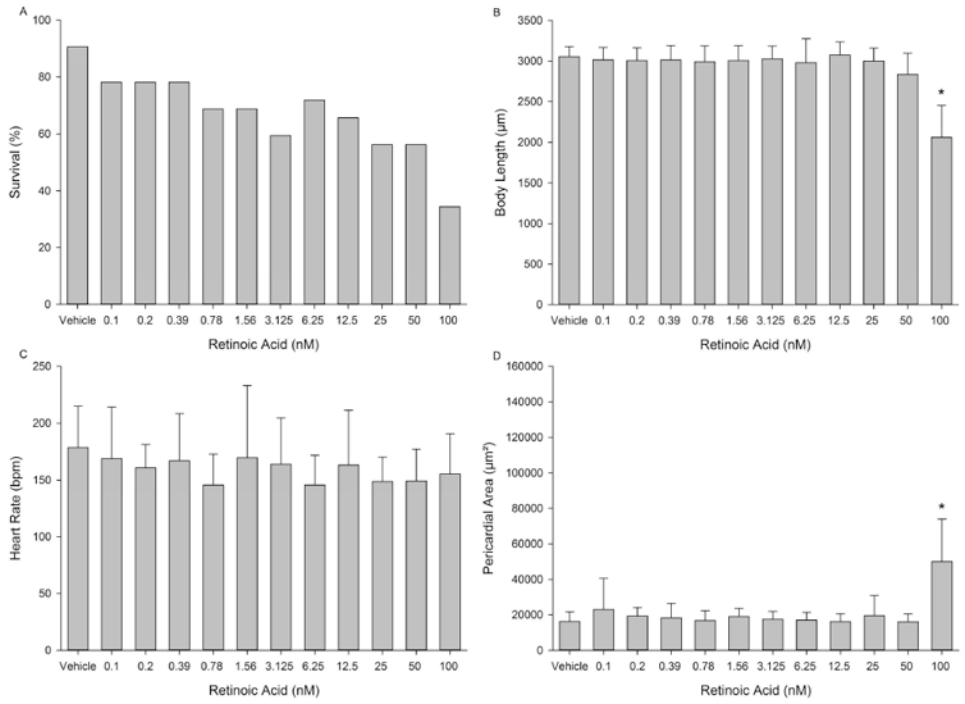

Figure 1.

Developmental toxicity of RA to 72-hpf zebrafish following static exposure from 5-72 hpf. (A) Embryo survival; (B) mean body length (± standard deviation); (C) mean heart rate (± standard deviation); and (D) mean pericardial area (± standard deviation). Asterisk (*) denotes significant treatment effect ($p<0.05$) relative to vehicle controls (0.1% DMSO). N = 32 initial embryos per control or treatment group.

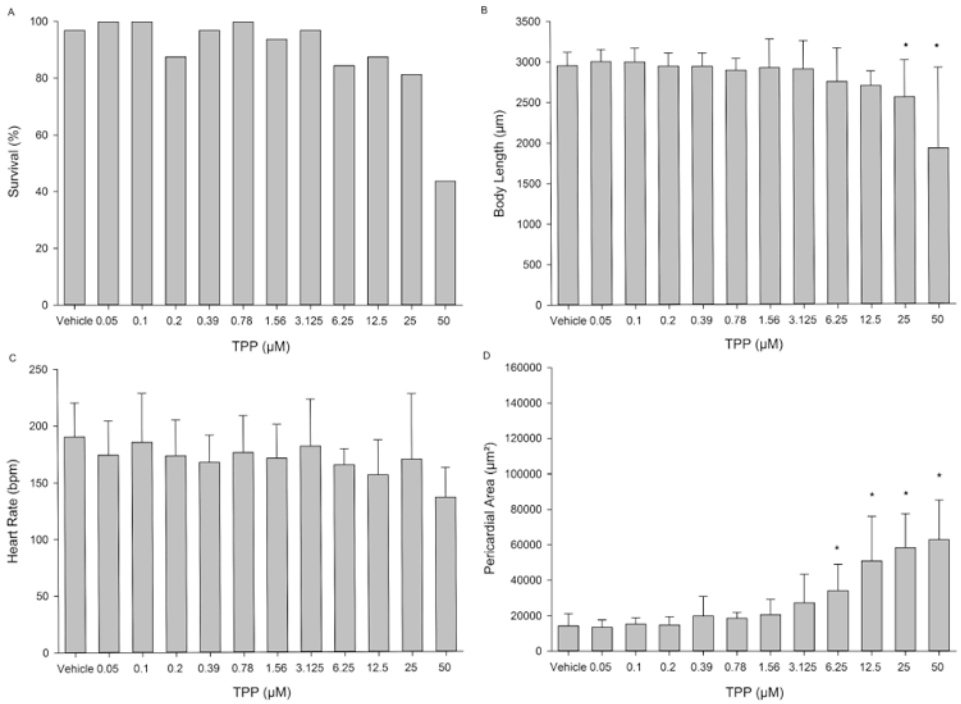

Figure 2.

Developmental toxicity of TPP to 72-hpf zebrafish following static exposure from 5-72 hpf. (A) Embryo survival; (B) mean body length (± standard deviation); (C) mean heart rate (± standard deviation); and (D) mean pericardial area (± standard deviation). Asterisk (*) denotes significant treatment effect ($p<0.05$) relative to vehicle controls (0.1% DMSO). N = 32 initial embryos per control or treatment group.

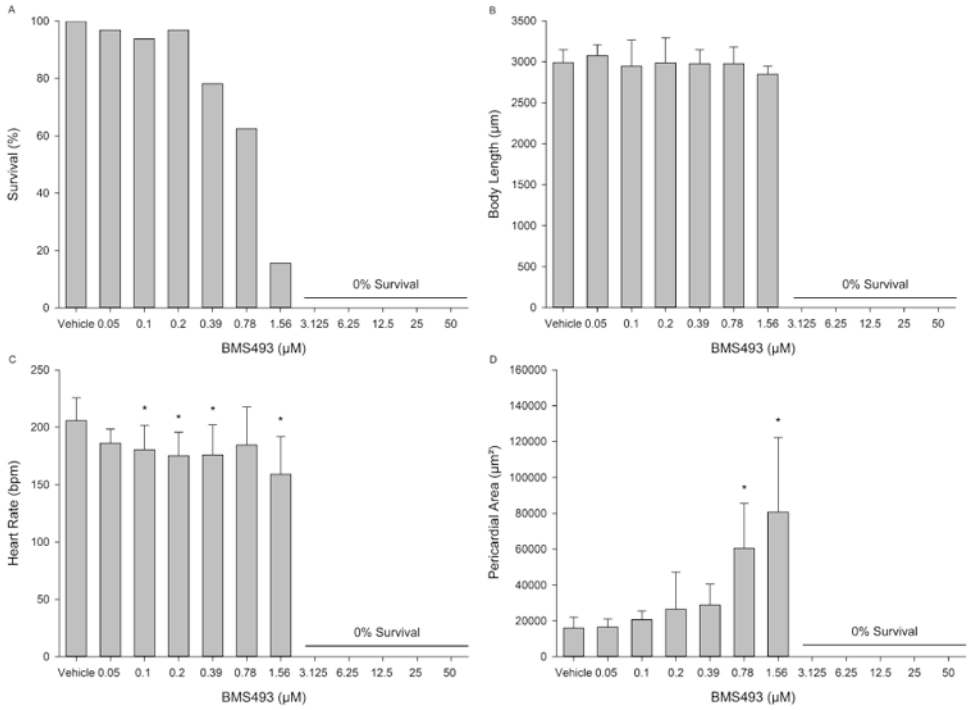

Figure 3.

Developmental toxicity of BMS493 to 72-hpf zebrafish following static exposure from 5-72 hpf. (A) Embryo survival; (B) mean body length (± standard deviation); (C) mean heart rate (± standard deviation); and (D) mean pericardial area (± standard deviation). Asterisk (*) denotes significant treatment effect ($p<0.05$) relative to vehicle controls (0.1% DMSO). N = 32 initial embryos per control or treatment group.

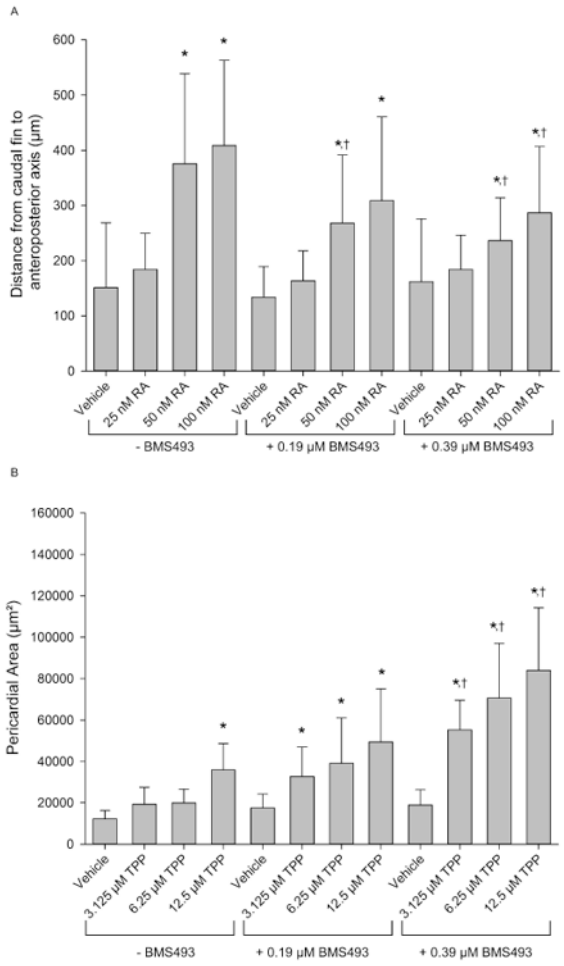

Figure 4.

BMS493 mitigates and enhances RA- and TPP-induced developmental toxicity, respectively, in zebrafish. (A) Mean distance (± standard deviation) from the caudal fin to the anteroposterior axis. (B) Mean pericardial area (± standard deviation). Asterisk (*) denotes significant treatment effect ($p<0.05$) relative to within-group vehicle controls (0.1% DMSO), whereas single cross (†) denotes significant effect ($p<0.05$) of BMS493 co-exposure relative to the same concentration of RA or TPP without BMS493. $N = 32$ initial embryos per control or treatment group.

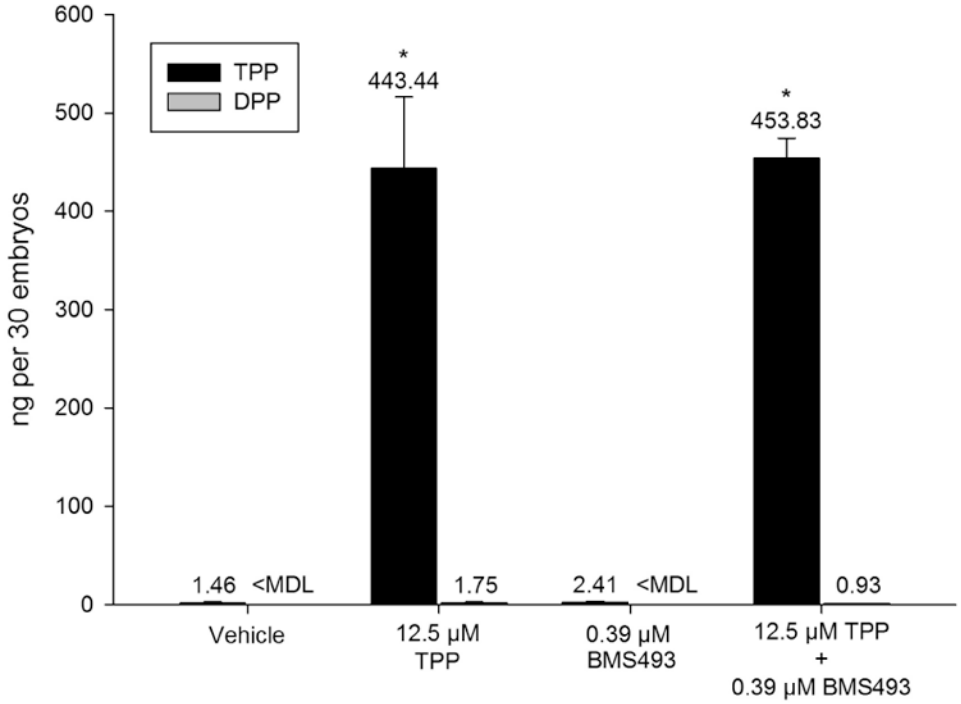

Figure 5.

BMS493 does not affect TPP uptake or metabolism to DPP. Mean (± standard deviation) dose (ng) of TPP or DPP detected in homogenates of 30 whole embryos exposed to vehicle (0.1% DMSO) or 12.5 µM TPP in the presence or absence of 0.39 µM BMS493. Asterisk (*) denotes significant treatment effect ($p<0.05$) relative to vehicle controls (0.1% DMSO). No significant differences in TPP or DPP were detected within the TPP-BMS493 co-exposure compared to TPP alone. *N* = three replicate pools per treatment. MDL = method detection limit.

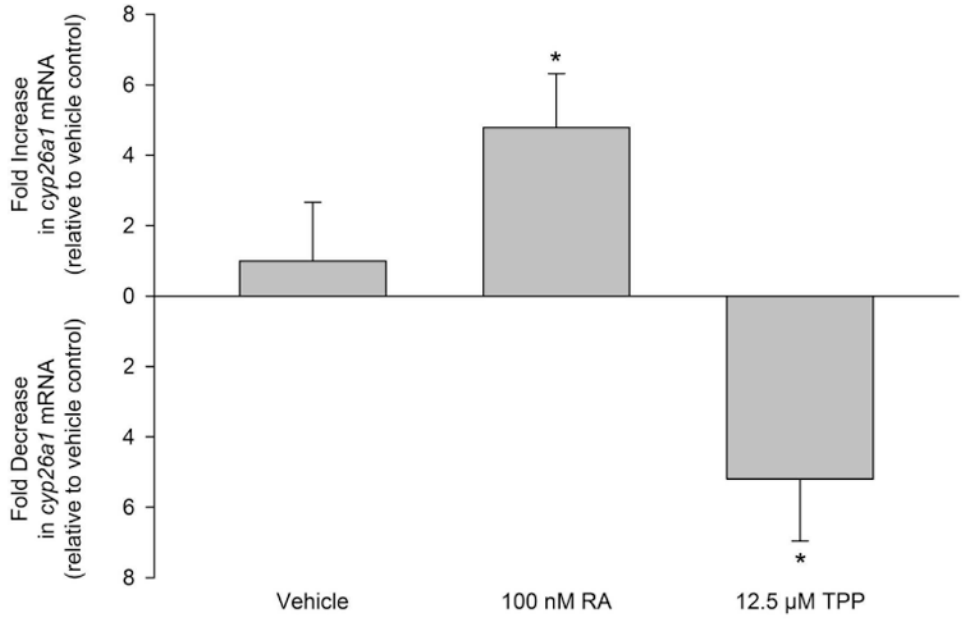

Figure 6.

RA and TPP exposure from 5-72 hpf results in increased and decreased *cyp26a1* expression, respectively, at 72 hpf. Mean fold change data (± standard deviation) are relative to *cyp26a1* expression within vehicle controls. Asterisk (*) denotes significant treatment effect ($p<0.05$) relative to vehicle controls. *N* = four RNA samples derived from four replicate pools of 60 72-hpf embryos per pool.

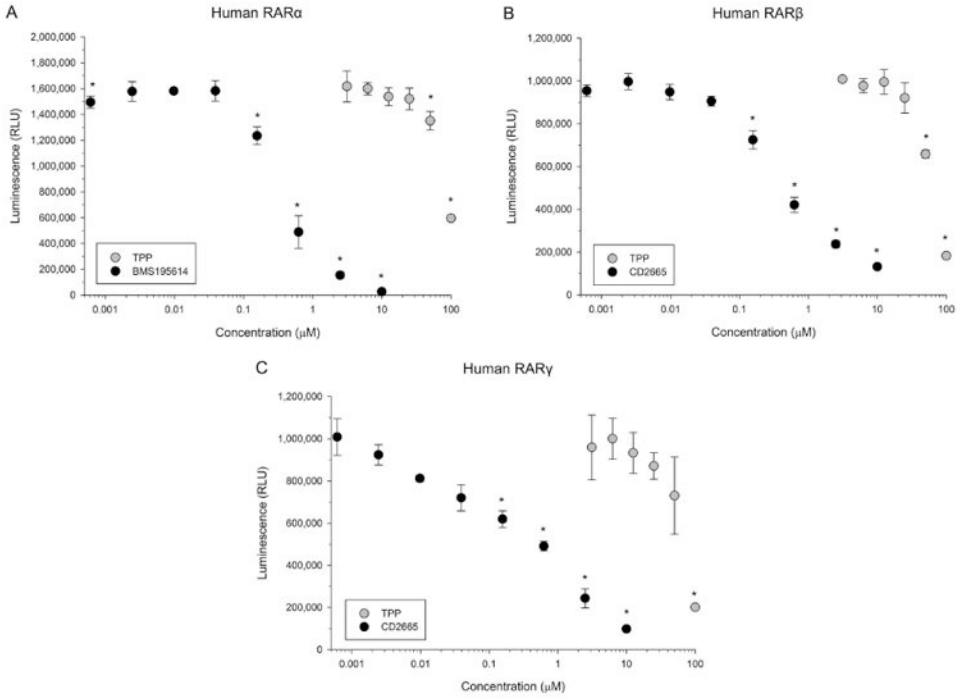

Figure 7.

TPP inhibits RA-induced activation of human RARα-, RARβ-, and RARγ. (A) Mean luminescence (± standard deviation) from human RARα-expressing and RA-activated Chinese hamster ovary cells following exposure to TPP or BMS195614 (reference RARα antagonist). (B) Mean luminescence (± standard deviation) from human RARβ-expressing and RA-activated Chinese hamster ovary cells following exposure to TPP or CD2665 (reference RARβ antagonist). (C) Mean luminescence (± standard deviation) from human RARγ-expressing and RA-activated Chinese hamster ovary cells following exposure to TPP or CD2665 (reference RARγ antagonist). Asterisk (*) denotes significant treatment effect ($p<0.05$) relative to vehicle controls (0.1% DMSO). *N* = three assay wells per control or treatment group.